Acoustical inverse methods for bone media identification with ultrasonic reflected waves

Rémi Roncen, Zine El Abiddine Fellah, Erick Ogam

ACOUSTICAL INVERSE METHODS FOR BONE MEDIA IDENTIFICATION WITH ULTRASONIC REFLECTED WAVES

R. Roncen[1] **Z.E.A. Fellah**[2] **E. Ogam**[2]

[1] ONERA/DMPE, Université de Toulouse, F-31055, Toulouse, France
[2] Laboratoire de Mecanique et d'Acoustique, CNRS, UMR 7031, Aix-Marseille Universite, Centrale Marseille, F-13402 Marseille Cedex 20, France

remi.roncen@onera.fr, fellah@lma.cnrs-mrs.fr

ABSTRACT

The non-intrusiveness and low cost of ultrasonic techniques are motivating the development of new means towards the detection of osteoporosis and other bone deficiencies. Bones are porous media saturated by a viscous fluid, and could thus be well characterized by the Biot model. The main purpose of this work is to present an in vitro methodology for bone identification, adopting a statistical Bayesian inference technique using ultrasonic reflected signals at normal incidence on human femoral bone samples.

1. INTRODUCTION

Osteoporosis affects the bone density and microstructure [1], reducing bone quality and increasing the risk of fractures. The bone mass density (BMD) can be evaluated by X-Ray absorptiometry, but the BMD alone does not fully account for fracture risks [2]. There is thus a need to refine the characterization of bones, to help better understand the onset of bone aging and deterioration, and improve the detection of bone diseases.

Biot's theory relates the microstructural and mechanical properties of poroelastic media to their acoustic behavior [3–9].

Using the Biot model, coupled with a model for the dissipation occurring within the pores, one can relate the microstructural and mechanical properties of the bone to its acoustic response. It then becomes possible to attempt an inverse problem, where the observation of a certain quantity (here an ultrasonic signal reflected by the bone sample) is used to infer the values of the parameters of interest.

Ultrasonic reflected waves are considered in this work at almost normal incidence on porous samples immersed in water. Only reflected waves are considered because in some cases, the observation of a transmitted wave is impossible due to the high dissipation of waves within the bone samples. A Bayesian inference approach is performed to update our state of belief (in the form of probability density functions) on the model parameters, which consist of the classical Biot parameters (density, Young's modulus, Poisson's ratio etc) and the intrinsic microstructure properties of the Horoshenkov pore model (mean pore size and standard deviation).

The model is recalled in Section 2. The experimental configuration used to obtain the ultrasonic reflected signals and the statistical Bayesian inference problem are succinctly introduced in Section 3. The inference method is then applied on experimental measurements of different bone samples extracted from human femoral head samples in Section 4. A conclusion is drawn in Section 5.

2. MODELING

In this work, we use Biot's alternative formulation [10], and take into account the additional visco-inertial dissipation that occurs within the pores, as developed by Horoshenkov [11]. The main reason for the use of the Horoshenkov model in the present work is the need for a set of identified parameters that are easily understandable by the medical community (i.e., the mean pore radius is potentially clearer than the viscous characteristic length of the Johnson-Koplik-Dashen (JKD) pore model [12], often used in the acoustic community). We then follow Niskanen et al. [13] for the calculation of the reflection coefficient of the material (consisting in all successive reflected waves : a first reflected wave that has not travelled within the material, and a succession of waves that have made it to the other end of the sample before coming back).

Biot's coupling equations are given in the harmonic domain as

$$\begin{aligned} \omega^2 \rho_f \boldsymbol{w} + \omega^2 \rho \boldsymbol{u} &= -\Delta \cdot \boldsymbol{\sigma}, \\ \omega^2 \rho_f \boldsymbol{u} + \omega^2 \tilde{\rho}_{\text{eq}} \boldsymbol{w} &= \Delta \cdot p, \end{aligned} \tag{1}$$

where p is the pressure field, $\boldsymbol{\sigma}$ is the total stress tensor, $\boldsymbol{u}$ is the solid phase displacement field, $\boldsymbol{w}$ is the relative displacement field between the phases. The angular frequency writes $\omega = 2\pi f$, with f the frequency in Hz; ρ_f is the ambient fluid density and $\rho = (1-\phi)\rho_s + \phi\rho_f$ is the density of the bulk medium, with ρ_s the density of the calcified tissue and ϕ the porosity. The equivalent density of the fluid phase $\tilde{\rho}_{\text{eq}}$ is a complex frequency dependent quantity that takes into account visco-inertial effects within the fluid phase inside the pores. The equivalent density is taken in this work as the one of Horoshenkov [12], based on the rational (Pad) approximation approach [14] and

on the hypothesis that the pore size follows a log-normal distribution and that the pores have a circular shape. In the case where the above approximations are valid, the Horoshenkov model for viscous dissipation writes

$$\tilde{\rho}_{\text{eq}} = \frac{\rho_f}{\phi}\tilde{\alpha}(\omega), \tag{2}$$

where the dynamic tortuosity $\tilde{\alpha}$ is defined as

$$\tilde{\alpha}(\omega) = \alpha_\infty \left[1 + \frac{1}{\mathrm{j}\bar{\omega}}\tilde{F}(\omega)\right], \tag{3}$$

with

$$\tilde{F}(\omega) = 1 - P + P\sqrt{1 + \frac{M_2}{2P^2}\mathrm{j}\bar{\omega}}, \quad \bar{\omega} = \omega\rho_f\frac{k_0\alpha_\infty}{\mu\phi}, \tag{4}$$

$$P = 4\frac{M_2}{2\beta_P\phi\Lambda^2}, \quad M_2 = 8\frac{k_0\alpha_\infty}{\phi\Lambda^2}. \tag{5}$$

The parameters used in this model are the classical JKD ones [12], and relate to the microstructure of the porous sample: porosity ϕ, tortuosity α_∞, permeability k_0 and characteristic viscous length Λ. Using the hypotheses of a log-normal pore distribution and a circular pore shape, it is possible to use only three parameters, namely the porosity ϕ, mean pore size $\bar{s}$ and pore size standard deviation σ_s (normalized by $\log(\bar{s})$), instead of four. The relationships between JKD and Horoshenkov model parameters are [15, 16]

$$\phi = \phi, \quad \alpha_\infty = e^{4(\sigma_s \log 2)^2},$$
$$k_0 = \frac{\bar{s}^2\phi}{8\alpha_\infty}e^{-6(\sigma_s \log 2)^2}, \quad \Lambda = \bar{s}e^{-\frac{5}{2}(\sigma_s \log 2)^2},$$
$$\beta_P = \frac{4}{3}e^{4(\sigma_s \log 2)^2}.$$

The presence of coupling between the fluid and solid phases in Eq. 1 is evidenced by the relationship between the total stress tensor $\boldsymbol{\sigma}$ and the pressure field p, which reads, for an isotropic porous material (at the wavelength scale), as

$$\boldsymbol{\sigma} = 2N\boldsymbol{\epsilon} + (\lambda_c\xi - \alpha_B M\zeta)\,\mathbb{I},$$
$$p = M\,(\zeta - \alpha_B\xi)\,, \tag{6}$$

where N is the shear modulus, $\boldsymbol{\epsilon}$ is the strain tensor, $\mathbb{I}$ is the identity matrix, (ξ is θ in Ref. [13]) and $\zeta = -\nabla\cdot\boldsymbol{w}$. The Biot-Willis coefficient α_B (α in Ref. [17, Eq. 28]) writes, after simplifications,

$$\alpha_B = 1 - \frac{K_b}{K_s}, \tag{7}$$

where K_b is the bulk modulus of the porous frame and K_s is that of the solid constituent of the material. The shear modulus N, the Young's modulus and Poisson's ratio of the solid E_s, ν_s and the bulk skeletal frame E_b, ν_b are related to the bulk moduli by

$$K_s = \frac{E_s}{3\,(1-2\nu_s)}, \quad K_b = \frac{E_b}{3\,(1-2\nu_b)}, \quad N = \frac{E_b}{2\,(1+\nu_b)}. \tag{8}$$

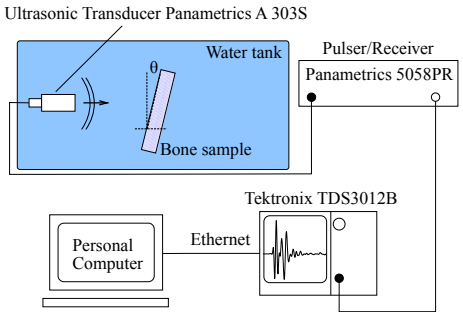

Figure 1: Experimental setup for ultrasonic measurements in a water tank

It is known [17, Eq. 28] that α_B is constrained by $\phi < \alpha_B$, i.e., $K_b < (1-\phi)K_s$.

In Eq. 6, λ_c is an elastic parameter defined as

$$\lambda_c = \lambda + \alpha_B^2 M, \tag{9}$$

with λ the first Lamé's coefficient of the elastic frame, and

$$M = \left[\alpha_B + \left(\frac{K_s}{K_f} - 1\right)\phi\right]^{-1} K_s, \tag{10}$$

with K_f the bulk modulus of the intra-pore fluid (water here, in which thermal effects can be neglected).

The analytical calculation in the frequency domain of the reflection coefficient $\mathcal{R}(\omega)$ of a bone sample is done by solving the system (1) and associated boundary conditions [18, Chap. 6]. We follow, as was done in Ref. [13, 19], the state vector formalism that makes it possible to write the motion equations as an ordinary differential equation, coupled to a global matrix approach to a solution for the Biot equations [20, 21]. Physical fields are expressed as a function of wave amplitudes, thus naturally introducing the transmission and reflection coefficients in the matrix representation. These coefficients are then extracted after the solving of a linear system, conveniently expressed with a sparse matrix easy to inverse at all frequencies simultaneously.

3. BAYESIAN INFERENCE

3.1 Experimental method

Experiments are performed in water using one Panametrics A 303S plane piezoelectric transducers of diameter $1\,\mathrm{cm}$, with a $500\,\mathrm{kHz}$ central frequency. $400\,\mathrm{V}$ pulses are provided by a 5058PR Panametrics pulser/receiver, amplified to $90\,\mathrm{dB}$, filtered above $10\,\mathrm{MHz}$ and averaged over 1000 iterations. A schematic of the experiment is shown in Fig. 1. The size of the ultrasound beam is small compared with the size of the specimens. The liquid initially in the pore space (blood and marrow) is removed from the bone sample and substituted by water. The bone samples, machined from the cancellous parts of a femoral head, are constantly immersed in liquid to prevent them from drying, which can alter their properties [22]. Due to possible manufacturing defects and positioning uncertainties, the angle of

incidence θ of the pressure wave (displayed in Fig. 1) is taken as an additional unknown.

3.2 Bayesian inference

In the context of statistical inverse problems, the Bayesian inference framework consists in recasting the model parameters of interest as random variables associated with probability densities encompassing the information one has on the parameters [23, Chap. 8]. A new experimental data v^{obs} is observed (here a reflection coefficient), and this information updates our state of knowledge. v^{obs} is the realization of a multivariate random variable Υ^{obs}. The degree of knowledge about the true value of the parameters $Q = (\phi, K_b, \ldots)$, with realizations q, is represented by the marginal posterior density $\pi(q|v^{\text{obs}})$. This new quantity of interest is written, using Bayes theorem,

$$\pi(q|v^{\text{obs}}) = \frac{\pi(v^{\text{obs}}|q)\,\pi_0(q)}{\pi(v^{\text{obs}})}. \tag{11}$$

In the previous equation, $L(q) \equiv \pi(v^{\text{obs}}|q)$ is the likelihood function, representing the probability that the experience be observed, given a particular set of model parameters; $\pi_0(q)$ is the prior probability, representing all the information obtained on q prior to the new observation (i.e, earlier measurements on the sample, or general knowledge of some of the bone properties such as its mineral density). Finally, $\pi(v^{\text{obs}})$ is a scaling constant not calculated in practice. Details on the likelihood and prior modeling are given in Refs. [13, 19].

Contrary to our previous work [19], we now use a frequency domain information to build the likelihood. It writes, when considering a Gaussian error representing the measurement uncertainties,

$$\pi(v_i^{\text{obs}}|q) = \pi_{\Re} \cdot \pi_{\Im}, \tag{12}$$

with

$$\pi_{\Re} = \prod_{i=1}^{n} \frac{1}{\sqrt{2\pi\sigma_{\Re,i}^2}} e^{-|\Re\left(v_i^{\text{obs}} - R_i(q)\right)|^2/2\sigma_{\Re,i}^2}$$

and a similar definition for $\pi_{\Im}$, where $n = 50$ is the number of discrete frequencies where the reflection coefficient was measured, and $R_i(q)$ is the numerical reflection coefficient. The noise parameter $\sigma_{\Re,i}$ (resp. $\sigma_{\Im,i}$) is a standard deviation of the assumed Gaussian distribution of errors on the real part (resp. imaginary part). This parameter is included in the inference process, but a single value σ is assumed at all frequencies and for both real and imaginary parts, since they have the same order of magnitude in most cases.

Contrary to the work of [13], only the reflection coefficient is used, not the transmission coefficient. The objective of this work is to evaluate the type of knowledge that can be extracted from this quantity only.

4. RESULTS

A numerical method is used in order to sample directly from the posterior density of interest $\pi(q|v^{\text{obs}})$, as detailed in previous work [19]. The strategy relies on the use of an evolutive Markov Chain Monte Carlo of Laloy et al. [24], shown to be efficient in sampling complex multimodal posterior densities. This multimodality, which was shown in [19], is a sign of ill-posedness: multiple solutions to the inverse problem exist. The parameters that are identified in this work, as well as the bounds of the uniform prior densities used during the inference, are given in Tab. 1. It was only possible to gain information on certain of the above properties, using only ultrasonic reflected signals. The general identification result, in the form of posterior probability densities (pdf), is shown in Fig. 2a, Fig. 3a and Fig. 4a for samples M_1, M_2, M_3. For each sample M_i, only the porosity ϕ, mean pore size and standard deviation $\bar{\sigma}, \sigma_s$, and skeletal frame Young modulus E_b are given. These are the parameters that could be inferred in the majority of the cases. No real gain of information could be obtained on the other parameters (except the noise parameter σ, the angle of incidence and sample thickness, which are of less interest to this study and are thus not shown).

Using the inferred parameters and their uncertainties, it is possible to recalculate the associated reflection coefficient, and to convoluate it with the incident signal (actually an inverse Fourier transform on the product between spectrum of the incident wave and reflection coefficient). One then obtains a reflected signal that can be compared to the experimental value measured on the oscilloscope. These are shown in Fig. 2b, Fig. 3b and Fig. 4b. A number of $N = 500$ samples are extracted from the pdfs, and the reflected signals are calculated N times. This allows us to plot uncertainties in Fig. 2b, Fig. 3b and Fig. 4b, where the darker area corresponds to a credibility interval of 63%, and the lighter area to a credibility interval of 95%, meaning that 63% (resp. 95%) of the samples are contained within.

Note that the bone samples come from different bones, and it is thus not expected that the same properties be inferred in each cases. However, for each sample, multiple measurements have been done at different site location for a repeatability study (shown in Fig. 2b, Fig. 3b and Fig. 4b, where the line style for the experimental signal corresponds to the results in Fig. 2a, Fig. 3a and Fig. 4a). Since the reflected signals are not exactly the same at each measurement location for a given sample, the inferred properties are not the same in all cases. This is partly explained by the known inhomogeneities present in bone samples.

The main conclusions drawn from the results in Fig. 2, Fig. 3 and Fig. 4 are that the identification is quite stable relative to the input signals. For the multiple measurements performed at different locations on each sample, the identified parameters are relatively close. While in some cases the pdfs are bi-modal (see Fig. 3 for E_b), one of the modes of the pdf is in the expected value range. The sensitivity of the parameters relatively to the identification is best seen with the pdfs having quite a restricted support, compared with the initial supports given by the priors in Tab. 1. This indicates that knowledge was extracted from the reflected signals. This is particularly important, since these identi-

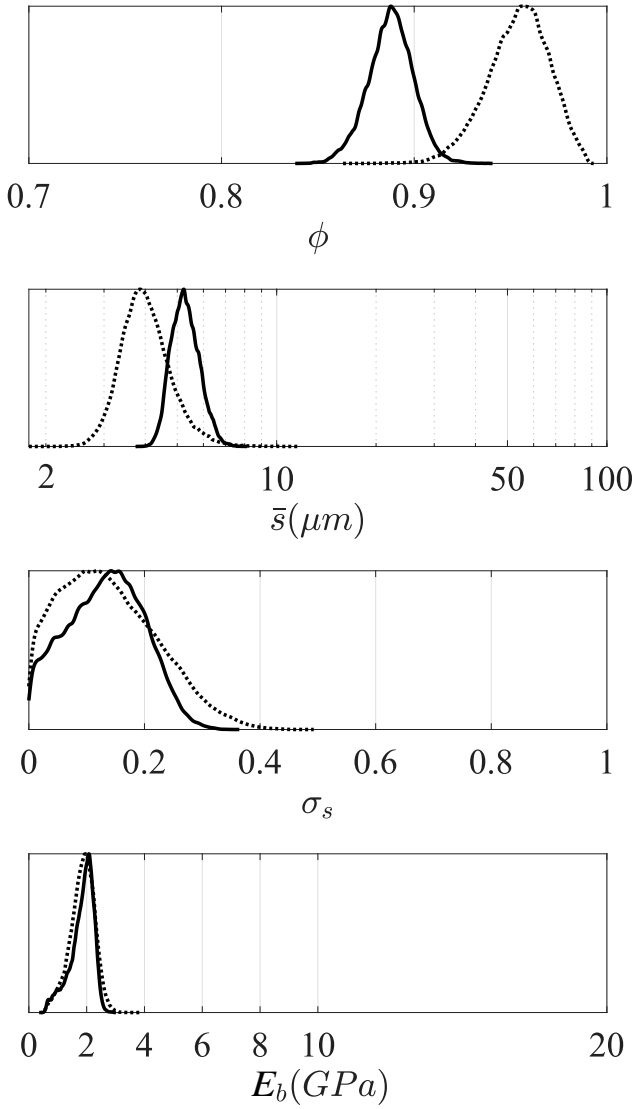

(a) Posterior marginal densities for material M_1

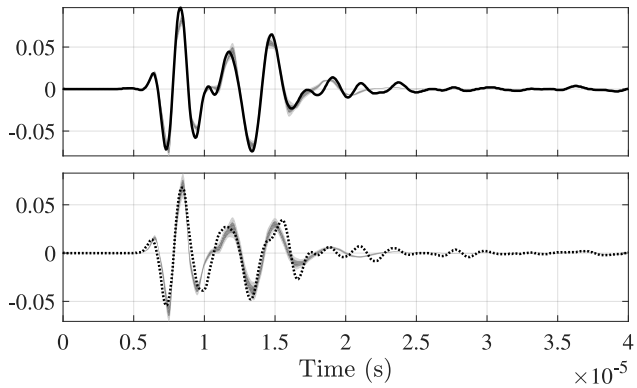

(b) Credibility intervals and experimental ultrasonic measurement for material M_1

Figure 2: Identification results for material M_1. Measured reflected signals were acquired at two different locations on the sample., each corresponding to a line style on the figure. The line type on both sub-figures correspond to the same inference.

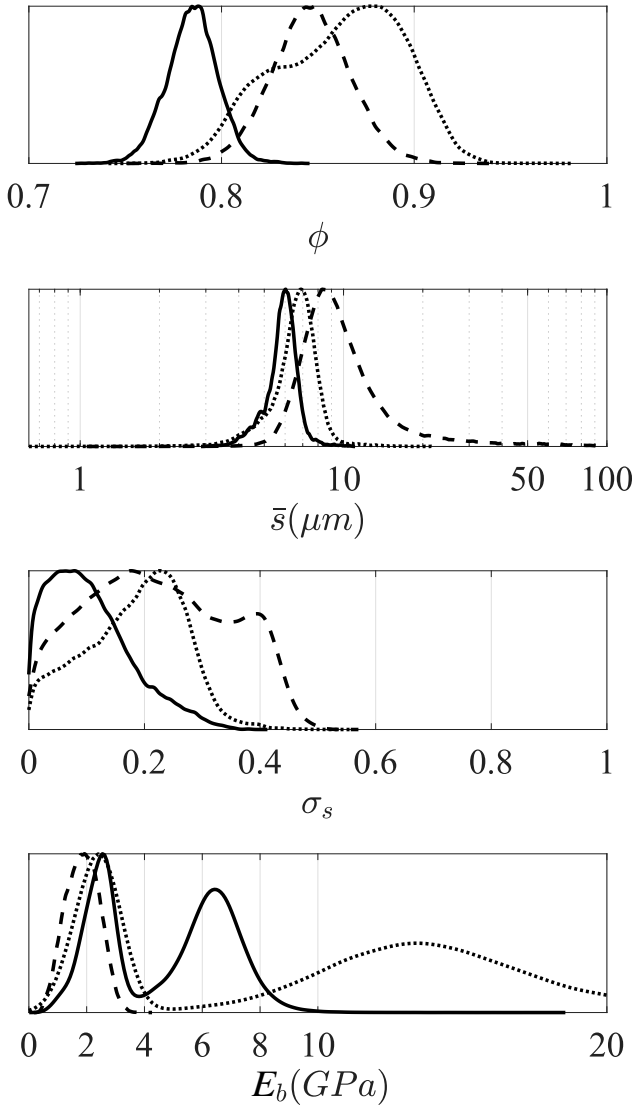

(a) Posterior marginal densities for material M_2

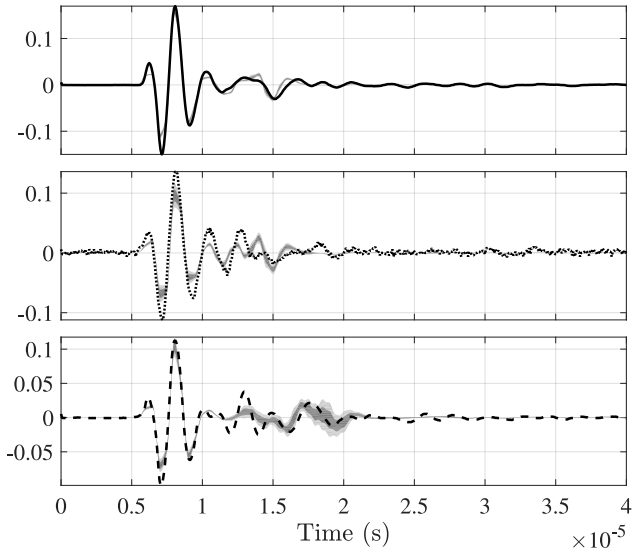

(b) Credibility intervals and experimental ultrasonic measurement for material M_2

Figure 3: Identification results for material M_2. Measured reflected signals were acquired at three different locations on the sample., each corresponding to a line style on the figure. The line type on both sub-figures correspond to the same inference.

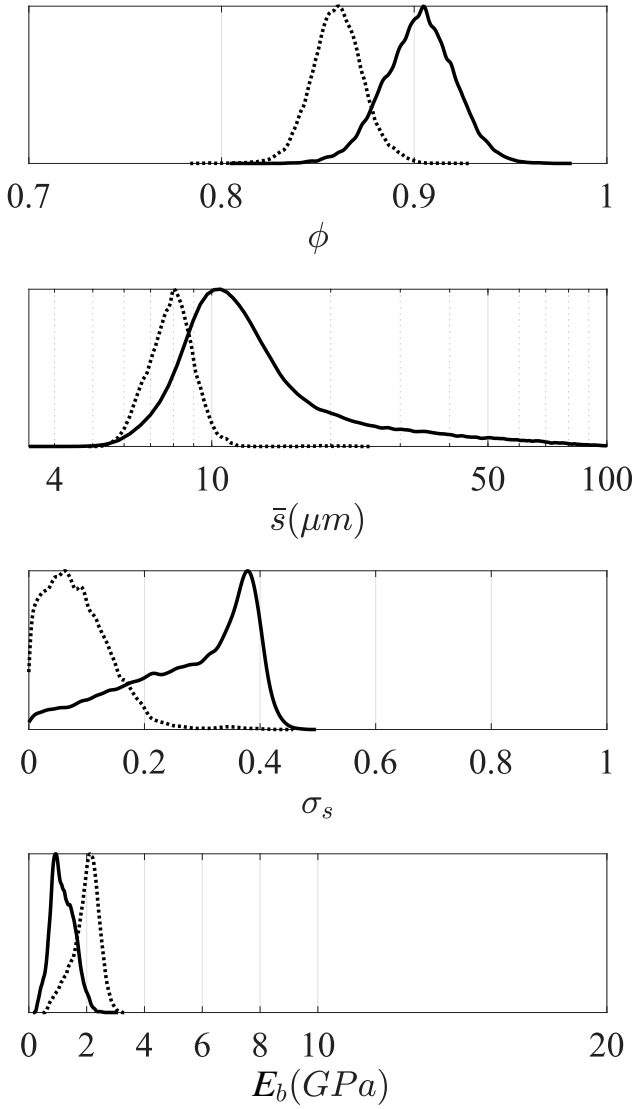

(a) Posterior marginal densities for material M_3

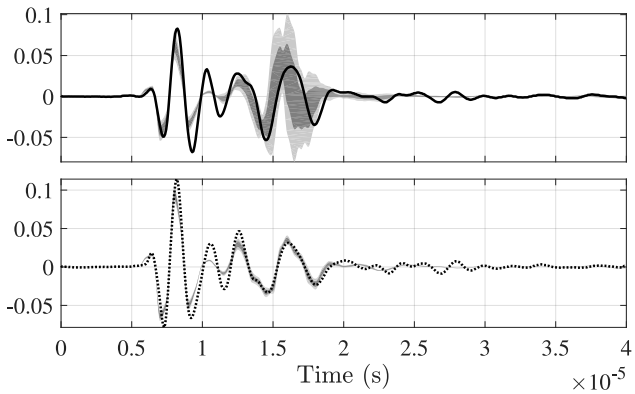

(b) Credibility intervals and experimental ultrasonic measurement for material M_3

Figure 4: Identification results for material M_3. Measured reflected signals were acquired at two different locations on the sample., each corresponding to a line style on the figure. The line type on both sub-figures correspond to the same inference.

Table 1: Prior bounds of the parameters for bone samples. The symbol – means unitless

	θ	L	ϕ	$\bar{s}$	σ_s	K_s	ξ_s	E_b/K_s	ξ_b	ν_b	ρ_s	K_f	μ_f	ρ_f
Unit	rad	mm	–	μm	/	GPa	–	GPa	–	–	$\mathrm{kg/m^3}$	GPa	$\mathrm{mPa \cdot s}$	$\mathrm{kg/m^3}$
$q_{\min}$	-0.05	$0.9L_i^*$	0.4	1.0	0	5	0	0.001	0	0.1	1.8	2.3	0.95	0.95
$q_{\max}$	0.05	$1.1L_i^*$	0.99	100	2	150	0.9	0.9	0.5	0.45	2.2	2.5	1.05	1.05

fied parameters could be promising in the detection of the onset of bone diseases, if the method can be ported to in-vivo measurements.

In all the cases treated in this work, the fit between the time domain signals was good (see Fig. 2b, Fig. 3b and Fig. 4b). While it is not a proof in itself that the identified parameters are the "correct" one, since there exists the possibility that part of the probability space was overlooked by the MCMC algorithm, this is an indicator of fitness that we can use to judge a solution. It has to be noted that the Bayesian inference was performed on frequency domain signals (reflection coefficient), and not on these time domain signals. Still, the main features of the signals are well captured in most cases.

5. CONCLUSION

This article has introduced a general identification method for in-vitro femoral head bone samples, based on ultrasonic reflected signals through bone samples saturated by water. A statistical inference strategy has been used to identify microstructural and mechanical properties of three porous samples. The advantage of this method is that it provides the uncertainty on the model parameters, and a robust way to take into account prior knowledge on the different identified properties, if any. It was possible to prove the robustness of the method by repeating the inference process on different signals obtained on the same samples. While ill-posedness was not an issue after regularization of a single parameter (the bone density), some parameters were not well identified due to their lack of sensitivity relative to the reflection coefficient. Still, the main parameters of interest were successfully identified. Future efforts should be dedicated to the taking into account of inhomogeneities in the width of the sample, to try and identify a field of properties, instead of a single value. At the time of the writing of this proceeding, an article has been submitted to JASA to present more results on different samples, and a numerical validation of the inference strategy.

6. ACKNOWLEDGMENT

This work has been conducted under the ONERA-CNRS collaboration agreement on porous media acoustics. The authors would like to thank Estelle Piot for her fruitful comments on this work.

7. REFERENCES

[1] R. Marcus, D. Feldman, D. Nelson, and C. J. Rosen, *Fundamentals of osteoporosis*. London: Academic Press, 4th ed., 2009.

[2] C.-C. Glüer and I. Q. U. C. Group, "Quantitative ultrasound techniques for the assessment of osteoporosis: expert agreement on current status," *Journal of Bone and Mineral Research*, vol. 12, no. 8, pp. 1280–1288, 1997.

[3] M. McKelvie and S. Palmer, "The interaction of ultrasound with cancellous bone," *Physics in Medicine & Biology*, vol. 36, no. 10, p. 1331, 1991.

[4] Z. E. A. Fellah, J. Y. Chapelon, S. Berger, W. Lauriks, and C. Depollier, "Ultrasonic wave propagation in human cancellous bone: Application of biot theory," *The Journal of the Acoustical Society of America*, vol. 116, no. 1, pp. 61–73, 2004.

[5] K. R. Marutyan, M. R. Holland, and J. G. Miller, "Anomalous negative dispersion in bone can result from the interference of fast and slow waves," *The Journal of the Acoustical Society of America*, vol. 120, no. 5, pp. EL55–EL61, 2006.

[6] E. R. Hughes, T. G. Leighton, P. R. White, and G. W. Petley, "Investigation of an anisotropic tortuosity in a biot model of ultrasonic propagation in cancellous bone," *The Journal of the Acoustical Society of America*, vol. 121, no. 1, pp. 568–574, 2007.

[7] M. Pakula, F. Padilla, P. Laugier, and M. Kaczmarek, "Application of biot's theory to ultrasonic characterization of human cancellous bones: determination of structural, material, and mechanical properties," *The Journal of the acoustical Society of america*, vol. 123, no. 4, pp. 2415–2423, 2008.

[8] G. Rus, M. Pakula, Q. Grimal, and P. Laugier, "Information theory framework to reconstruct biot constants of trabecular bone from ultrasound," in *2015 6th European Symposium on Ultrasonic Characterization of Bone*, pp. 1–4, June 2015.

[9] H. Chen, R. P. Gilbert, and P. Guyenne, "A biot model for the determination of material parameters of cancellous bone from acoustic measurements," *Inverse Problems*, vol. 34, no. 8, p. 085009, 2018.

[10] M. A. Biot, "Mechanics of deformation and acoustic propagation in porous media," *J. Appl. Acoust.*, vol. 33, no. 4, pp. 1482–1498, 1962.

[11] K. Horoshenkov and M. Swift, "The acoustic properties of granular materials with pore size distribution close to log-normal," *The Journal of the Acoustical Society of America*, vol. 110, no. 5, pp. 2371–2378, 2001.

[12] D. L. Johnson, J. Koplik, and R. Dashen, "Theory of dynamic permeability and tortuosity in fluid-saturated porous media," *J. Fluid Mech.*, vol. 176, pp. 379–402, 1987.

[13] M. Niskanen, O. Dazel, J.-P. Groby, A. Duclos, and T. Lähivaara, "Characterising poroelastic materials in the ultrasonic range-a bayesian approach," *Journal of Sound and Vibration*, vol. 456, pp. 30–48, 2019.

[14] K. V. Horoshenkov, K. Attenborough, and S. Chandler-Wilde, "Padé approximants for the acoustical properties of rigid frame porous media with pore size distributions," *The journal of the acoustical society of America*, vol. 104, no. 3, pp. 1198–1209, 1998.

[15] K. V. Horoshenkov, A. Hurrell, and J.-P. Groby, "A three-parameter analytical model for the acoustical properties of porous media," *The Journal of the Acoustical Society of America*, vol. 145, no. 4, pp. 2512–2517, 2019.

[16] K. V. Horoshenkov, A. Hurrell, and J.-P. Groby, "Erratum: A three-parameter analytical model for the acoustical properties of porous media [j. acoust. soc. am. 145 (4), 2512–2517 (2019)]," *The Journal of the Acoustical Society of America*, vol. 147, no. 1, pp. 146–146, 2020.

[17] M. Biot and D. Willis, "The elastic coefficients of the theory of consolidation," *J. appl. Mech*, vol. 24, pp. 594–601, 1957.

[18] J. Allard and N. Atalla, *Propagation of Sound in Porous Media: Modelling Sound Absorbing Materials 2e*. New York: John Wiley & Sons, 2009.

[19] R. Roncen, Z. Fellah, E. Piot, and E. Ogam, "Bayesian inference of a human bone and biomaterials using ultrasonic transmitted signals," *The Journal of the Acoustical Society of America*, vol. 146, no. 3, pp. 1629–1640, 2019.

[20] G. Gautier, L. Kelders, J.-P. Groby, O. Dazel, L. De Ryck, and P. Leclaire, "Propagation of acoustic waves in a one-dimensional macroscopically inhomogeneous poroelastic material," *The Journal of the Acoustical Society of America*, vol. 130, no. 3, pp. 1390–1398, 2011.

[21] O. Dazel, J.-P. Groby, B. Brouard, and C. Potel, "A stable method to model the acoustic response of multilayered structures," *Journal of Applied Physics*, vol. 113, no. 8, p. 083506, 2013.

[22] S. B. Lang, "Ultrasonic method for measuring elastic coefficients of bone and results on fresh and dried bovine bones," *IEEE Transactions on Biomedical Engineering*, no. 2, pp. 101–105, 1970.

[23] R. C. Smith, *Uncertainty quantification: theory, implementation, and applications*, vol. 12. Philadelphia: Siam, 2013.

[24] E. Laloy and J. A. Vrugt, "High-dimensional posterior exploration of hydrologic models using multiple-try dream(zs) and high-performance computing," *Water Resour. Res.*, vol. 48, no. 1, pp. n/a–n/a, 2012. W01526.